

## Determination of the Phase Difference between Even and Odd Continuum Wave Functions in Atoms through Quantum Interference Measurements

Zheng-Min Wang<sup>1,2</sup> and D. S. Elliott<sup>2</sup>

<sup>1</sup>*Department of Physics, Purdue University, West Lafayette, Indiana 47907*

<sup>2</sup>*School of Electrical and Computer Engineering, Purdue University, West Lafayette, Indiana 47907*

(Received 14 May 2001; published 4 October 2001)

We establish a technique for the determination of the phase difference between even and odd parity continuum wave functions in atoms. This determination is based upon our detailed measurements of a quantum mechanical interference between two photoionization processes using a two-color laser field. We present our measurement of the phase difference between the continuum  $p$  and  $d$  waves in atomic rubidium, which is in good agreement with the expected value.

DOI: 10.1103/PhysRevLett.87.173001

PACS numbers: 32.80.Qk, 32.10.-f, 32.80.Rm

We report our experimental determination of the phase difference between two continuum states that have the opposite parity, namely, the  $p$  and  $d$  waves in atomic rubidium. While several groups have previously measured the phase difference between atomic continuum states [1–7], these measurements have, until now, been restricted to states that have the same parity. By bridging the gap between the even and odd free atomic states, this technique allows a determination of the phase difference between any two continuum wave functions of an atom.

In conventional multiphoton ionization measurements, the atom absorbs the same number of photons to reach any continuum energy state, so that dipole selection rules restrict the parity of the final state to either even or odd, but not both. In contrast, the present determination is based upon measurements carried out with a phase-coherent two-frequency laser field, one component ionizing the atom through a linear interaction, the other through a two-photon process. Since the two field components can each independently photoionize the atom, an interference between the two interactions results, manifesting itself in an asymmetric angular distribution of the photoelectrons.

Demonstrations of the interference between even- and odd-order processes have been reported previously, including control over the photoelectron angular distribution (PAD) in atomic [8,9] or molecular [10] photoionization processes, control over the angular distribution of the

products in molecular photodissociation [11], and control over directional photocurrents in semiconductor materials [12,13]. In a recent theoretical work [14], Nakajima proposed a method of determining phase differences between even and odd continuum states using a two-pathway interference process. Our present measurements are based on the two-pathway interference, similar to Nakajima's scheme.

We consider photoionization of the atoms by the following two-frequency laser field:

$$\vec{E}(\vec{r}, t) = \{E_0^\omega \hat{z} \exp[-i(\omega t - \beta^\omega y - \phi^\omega)] + E_0^{2\omega} \hat{x} \exp[-i(2\omega t - \beta^{2\omega} y - \phi^{2\omega})]\} + \text{c.c.}, \quad (1)$$

where  $E_0^\omega$  and  $E_0^{2\omega}$  are the amplitudes of the fundamental frequency ( $\omega$ ) and second-harmonic ( $2\omega$ ) components of the laser field, respectively,  $\phi^\omega$  and  $\phi^{2\omega}$  are the phases of these optical waves, and  $\beta^\omega = n^\omega \omega/c$  and  $\beta^{2\omega} = n^{2\omega} 2\omega/c$  are their wave numbers. The ultraviolet ( $2\omega$ ) beam is polarized along the  $\hat{x}$  direction (horizontal), and the visible ( $\omega$ ) beam is polarized in the  $\hat{z}$  direction (vertical). One can extend the theoretical exposition of multiphoton ionization of atoms presented by Bebb and Gold [15] to include excitation by this two-frequency laser field, producing a photoelectron angular flux in the direction  $(\Theta, \Phi)$  of

$$W(\Theta, \Phi) = \frac{m|k|}{8\pi^2\hbar} \sum_{i,j=+/-} \left| \frac{eE_0^{2\omega} \exp(i\phi^{2\omega})}{2\hbar} O_{ij}^{(1)} + \frac{e^2(E_0^\omega)^2 \exp(2i\phi^\omega)}{2\hbar^2} T_{ij}^{(33)} \right|^2, \quad (2)$$

where  $O_{ij}^{(p)}$  and  $T_{ij}^{(pq)}$  are the spatial components of the one- and two-photon transition moments, respectively. The indices  $i, j = +$  or  $-$  of the moments  $O_{ij}^{(p)}$  or  $T_{ij}^{(pq)}$  represent the spin of the ground and the final state electron, respectively, and  $p, q = 1$  or  $3$  represent the spatial components. The moments relevant to our experiment are

$$O_{++}^{(1)} = \frac{-4\pi i}{\sqrt{6}} e^{i\xi_p} \left\{ -Y_{11} R_{3/2} + Y_{1-1} \left( \frac{R_{3/2} + 2R_{1/2}}{3} \right) \right\}, \quad (3a)$$

$$O_{+-}^{(1)} = \frac{-4\pi i}{\sqrt{3}} e^{i\xi_p} Y_{10} \left( \frac{R_{3/2} - R_{1/2}}{3} \right), \quad (3b)$$

$$T_{++}^{(33)} = \frac{1}{3} e^{i\xi_s} Y_{00} S_{\bar{s}} - \frac{2}{3\sqrt{5}} e^{i\xi_d} Y_{20} S_{\bar{d}}, \quad (3c)$$

$$T_{+-}^{(33)} = \sqrt{\frac{2}{15}} e^{i\xi_d} Y_{21} S_{\Delta d}. \quad (3d)$$

In these equations, the  $R_J$  represent the reduced single-photon transition moments from the ground state to the continuum  $\varepsilon p^2 P_J$  wave, where  $J = 3/2$  or  $1/2$ . The parameters  $S$  represent reduced two-photon transition moments for excitation of the  $s$  and  $d$  waves, and are defined in full in [7]. Briefly,  $S_{\bar{s}}$  is the average moment for excitation of the  $s$  wave,  $S_{\bar{d}}$  is the average moment for excitation of the  $d$  wave, and  $S_{\Delta d}$  is the asymmetry in the moments for excitation of the  $d$  wave. The phases  $\xi_s$ ,  $\xi_p$ , and  $\xi_d$  are the asymptotic phases of the continuum wave functions [16,17]. The  $--$  ( $-+$ ) component is obtained from the  $++$  ( $+--$ ) component for the  $O_{ij}^{(1)}$  terms by changing the spherical harmonic functions  $Y_{lm} \rightarrow -Y_{l-m}$ , and  $Y_{lm} \rightarrow Y_{l-m}$  for the  $T_{ij}^{(33)}$  terms.

We find it convenient to quantify the phase difference between the outgoing waves in terms of the phase

$$\delta_{pd} = (\phi^{2\omega} - 2\phi^\omega) + (\xi_p - \xi_d). \quad (4)$$

From Eqs. (2) and (3) we see that, up to an additional phase of  $-\pi/2$ , this phase represents the phase difference between the outgoing  $\varepsilon p^2 P, m_l = 1, m_s = 1/2$  and  $\varepsilon d^2 D, m_l = 0, m_s = 1/2$  waves. The phase of the  $s$  wave is, of course, also critical in these measurements, but since (i) we have previously determined  $\xi_s - \xi_d$  [7] and (ii) the cross section for excitation of the  $s$  wave is much smaller than that of the  $d$  wave, we report  $\xi_p - \xi_d$  as the primary result of this determination.

In Fig. 1 we show several examples of these photoelectron angular distributions, plotted on the basis of Eqs. (2) and (3). In each case the distance from the origin to the surface represents the photoelectron flux ejected in that direction. The first two figures are examples that might result for (a) noninterfering single-photon ionization by a horizontally polarized UV laser beam (a  $p$  wave, of odd parity) and (b) noninterfering two-photon ionization by a vertically polarized visible laser beam (a combination of  $s$  and  $d$  waves, both of even parity). When the atom is excited by both fields concurrently, a linear combination of even and odd parity waves is excited, and this superposition wave can be highly asymmetric. We show two examples of these angular distributions in Figs. 1(c) and 1(d). The amplitudes and polarizations of the individual field components are the same for these PADs as those

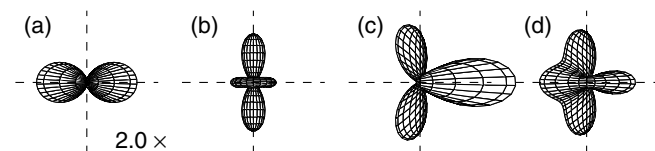


FIG. 1. Four examples of PAD calculated from Eq. (2). (a),(b) The PAD for single-photon ionization by a horizontally polarized laser beam and the PAD for two-photon ionization by a vertically polarized beam, respectively. The PADs in (c) and (d) show the result of the interference between the two concurrent interactions.

producing the noninterfering PADs in 1(a) and 1(b). The only difference between the fields producing the PADs in 1(c) and 1(d) is an increment of  $\delta_{pd}$  by  $90^\circ$ . The major contribution to the asymmetric distributions we observe is due to the interference between the opposing maxima of the  $p$  wave with the ring about the waist of the  $d$  wave.

We carry out the experiment using the apparatus shown schematically in Fig. 2. A single pulsed, tunable, dye laser and two-stage amplifier, pumped by the second-harmonic output of a Nd:YAG laser, generate a vertically polarized,  $\sim 10$  nsec duration, optical pulse at a wavelength of  $\lambda = 560$  nm and pulse energy of 2 mJ. We pass the beam through a spatial filter to improve its transverse mode structure, and split the beam into two components at the input beam splitter of a configuration similar to a Mach-Zehnder interferometer. In one branch of this configuration we insert a type-I phase-matched second-harmonic generating crystal (beta-barium borate, or BBO), which produces a horizontally polarized, phase-coherent pulse at a wavelength of  $\lambda/2 = 280$  nm and a pulse energy of  $12 \mu\text{J}$ . We match the optical length of the other branch of the Mach-Zehnder-like setup to that of the first to ensure that the propagation delay of the visible beam matches that of the UV beam when the two beams are recombined at the second beam splitter. Upon recombination, we must also ensure that the two laser beams are overlapped and parallel to better than  $0.05$  mrad. Otherwise the phase variation between the two beams differs across the interaction region, rendering the interference unobservable. We carefully match the beam sizes in the interaction region, and measure  $w = 0.7$  mm for the visible beam and  $w = 0.5$  mm for the ultraviolet beam, where  $w$  is the beam radius at which the intensity decreases to  $e^{-2}$  of the on-axis intensity. For perfectly Gaussian beams, the optimal ratio of the beam radii is  $\sqrt{2}$ .

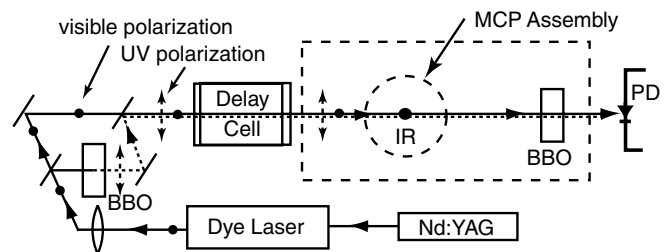


FIG. 2. A top view of the experimental setup. The elements are labeled as follows: BBO, second-harmonic generating crystals; IR, interaction region; PD, photodiode; MCP assembly, the photoelectron detector, consisting of a pair of parallel, biased meshes, a microchannel plate electron multiplier, and a phosphor screen. The vertically polarized fundamental beam (2 mJ pulse energy at  $\lambda = 560$  nm) is shown as a solid line, while the horizontally polarized harmonic beam ( $12 \mu\text{J}$  at  $\lambda = 280$  nm) is dashed. The offset shown between these two beams is for clarity only, as these two beams are precisely overlapped in the experiment. Each element inside the rectangular dashed line is contained within the vacuum chamber.

We direct the recombined beam through a variable density  $N_2$  delay cell and into the atomic beam apparatus, where it crosses a beam of atomic rubidium. The atomic beam, of density  $\sim 7 \times 10^7 \text{ cm}^{-3}$ , is produced by an effusive oven of temperature  $152^\circ\text{C}$ . Varying the density of  $N_2$  in the delay cell allows us to vary  $(\phi^{2\omega} - 2\phi^\omega)$ , with a change in pressure of 102 torr resulting in a  $2\pi$  phase shift. A second BBO crystal mounted inside the vacuum system allows us to calibrate the phase difference of the optical field components on an absolute (modulus  $2\pi$ ) basis [8]. The net second-harmonic field amplitude detected by the photodiode shown in Fig. 2 is the coherent sum of the fields generated in the first and second crystals, resulting in a sinusoidal dependence of the harmonic power at the photodiode on the  $N_2$  pressure. Since the BBO crystal is phase matched for second-harmonic generation, a maximum in this net harmonic power corresponds to a zero phase difference between the visible and UV fields in the interaction region.

We have described our detector in detail in a previous publication [7]. Briefly, it is an adaptation of that introduced by Helm *et al.* [18], in which the interaction region is situated between two parallel, biased meshes. A small dc electric field projects the photoelectrons upward onto a microchannel plate (MCP) electron multiplier and phosphor screen. The image of the photoelectrons is detected on a shot-by-shot basis by a digital camera interfaced to a personal computer. Under the conditions of our experiment, approximately 30 electrons are generated for each laser pulse. We generate a composite image by accumulating the data over 3000 laser pulses. We show several examples of the complete photoelectron images in Figs. 3(a1)–3(e1). We also plot a single row of

these same data (solid data points) in Figs. 3(a2)–3(e2), shown with the best theoretical fit to these data as the solid line. We determine this fit by mapping the parabolic trajectory of the photoelectrons ejected at an angle  $(\Theta, \Phi)$  from the interaction region onto the phosphor screen.

For the data shown in Figs. 3(a) and 3(b) we ionized the atoms with only one frequency component of the laser field at a time, Fig. 3(a) corresponding to one-photon ionization by the horizontally polarized UV light by itself and Fig. 3(b) from two-photon ionization by the vertically polarized visible light. The fitting procedure applied to the image data in Fig. 3(a1) yields the ratio  $R_{1/2}/R_{3/2} = 1.96$ , necessary for quantifying the one-photon contribution to the interference. To compute an image for comparison with the measured two-photon image shown in Fig. 3(b1), we use  $S_{\bar{s}}/S_{\bar{d}} = -0.42$ ,  $S_{\Delta d}/S_{\bar{d}} = -0.36$ , and  $\xi_s - \xi_d = 2.08$ , as determined at  $\lambda = 560 \text{ nm}$  in previous measurements [7].

In Figs. 3(c)–3(e), we show examples of data collected when both laser fields are incident concurrently upon the atom beam. The only parameters we adjusted to fit the two-color images were the relative phase difference between the waves,  $\delta_{pd}$ , and the amplitudes of the two terms in Eq. (2). The agreement between experimental data and fits is uniformly good. The quality of the theoretical fits to the experimental images is especially satisfying when we consider that no incoherent (noninterfering) terms are included in Eq. (2). These incoherent terms could conceivably arise during an experiment via a poor matching of the beam sizes or beam shapes of the two laser field components, or through imperfect alignment of the wave fronts of these beams.

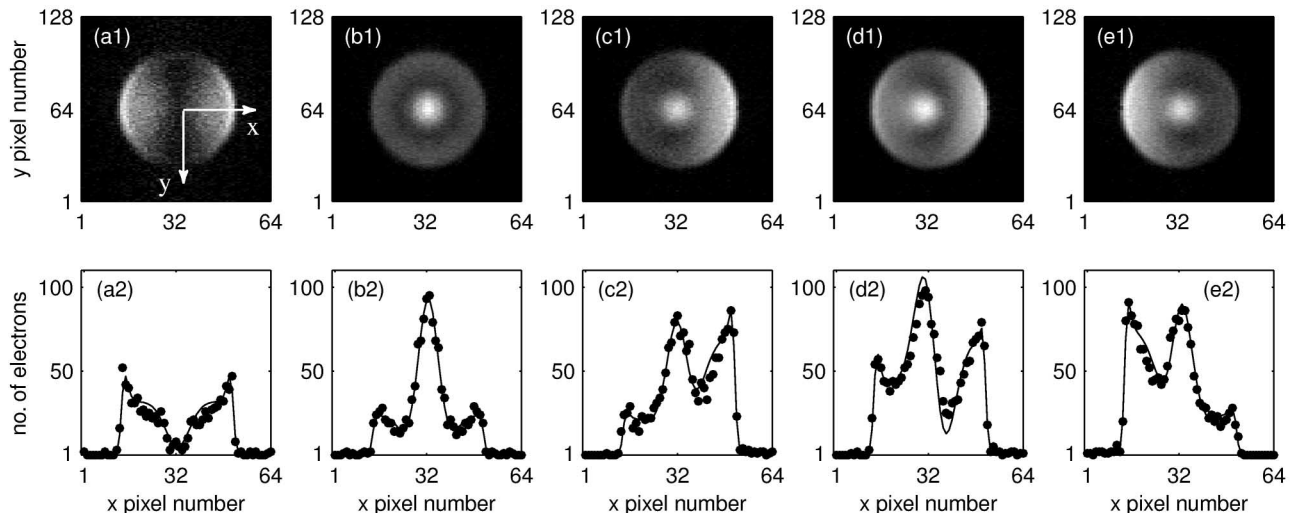


FIG. 3. Examples of the photoelectron images. The data shown in each column correspond to (a) one-photon ionization with horizontally polarized light alone, (b) two-photon ionization with vertically polarized light alone, and (c)–(e) ionization resulting from the interference between the two interactions. For each data set, we show (top) an image of the photoelectron distribution on the phosphor screen, and (bottom) a line plot showing a single row (row 64) of the data from the image. The solid lines are the best-fit calculated data. The laser beam propagates in the  $y$  direction, with the  $x$ - $y$  axes shown in (a1).

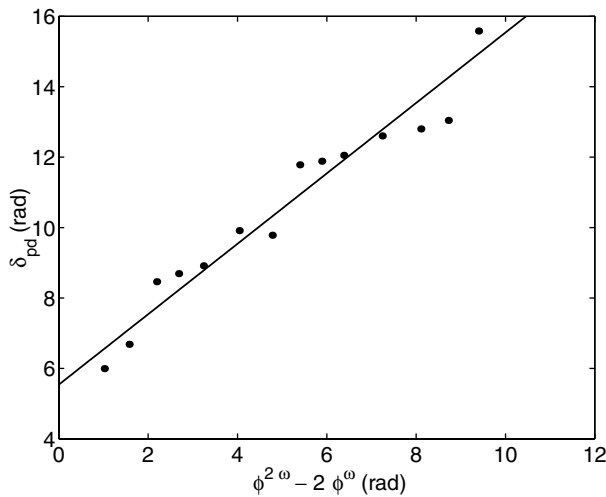


FIG. 4. The phase difference between the partial waves  $\delta_{pd}$  versus the optical phase difference  $2\phi^\omega - \phi^{2\omega}$ . The intercept of this plot yields the difference in scattering phase between the  $p$  and  $d$  waves.

In Fig. 4 we plot the phase difference  $\delta_{pd}$  that produces the best fit to the experimental images for fourteen different values of the optical phase difference  $\phi^{2\omega} - 2\phi^\omega$ . The solid line represents the best-fit straight line of unit slope for these data. An intercept of  $\xi_p - \xi_d = 5.54$  (modulus  $2\pi$ )  $\pm 0.18$  on this plot is our final result for the difference in the phases between these atomic  $p$  and  $d$  wave functions. We determine the uncertainty from the deviation of the data points in Fig. 4 from the straight line. For comparison, we can evaluate the expected value of this phase difference by using quantum defect data from the bound state spectra for the rubidium  $p$  and  $d$  rydberg series [19,20], combined with the analytic form of the Coulomb phase [16,17], yielding  $\xi_p - \xi_d = (1.301 - 0.958\varepsilon - 3.05\varepsilon^2)\pi + \arctan[1/(2\sqrt{\varepsilon})]$ , where  $\varepsilon$  is the photoelectron kinetic energy in rydbergs. At a photoelectron energy of  $\varepsilon = 0.0184$  Ry, corresponding to the wavelength of our laser source, the result of this evaluation is 5.334, in good agreement with our determination.

In conclusion, we have developed a method for determining the phase difference between even and odd continuum wave functions. This method, based on interference between two photoionization pathways, extends our capability for measuring phase differences to include any pair of atomic continuum states. The agreement between our computed images and the measured images is very good.

This material is based upon work supported by the National Science Foundation under Grant No. 9732611-PHY.

- 
- [1] J. A. Duncanson, Jr., M. P. Strand, A. Lindgård, and R. S. Berry, Phys. Rev. Lett. **37**, 987 (1976); J. C. Hansen, J. A. Duncanson, Jr., R.-L. Chien, and R. S. Berry, Phys. Rev. A **21**, 222 (1980).
  - [2] A. Siegel, J. Ganz, W. Bußert, and H. Hotop, J. Phys. B **16**, 2945 (1983).
  - [3] H. Kaminski, J. Kessler, and K. J. Kollath, Phys. Rev. Lett. **45**, 1161 (1980).
  - [4] U. Heinzmann, J. Phys. B **13**, 4353 (1980); Ch. Heckenkamp, F. Schäfers, G. Schönhense, and U. Heinzmann, Phys. Rev. Lett. **52**, 421 (1984); Z. Phys. D **2**, 257 (1986).
  - [5] A. Hausmann, B. Kämmerling, H. Kossmann, and V. Schmidt, Phys. Rev. Lett. **61**, 2669 (1988).
  - [6] K. L. Reid, D. J. Leahy, and R. N. Zare, Phys. Rev. Lett. **68**, 3527 (1992).
  - [7] Zheng-Min Wang and D. S. Elliott, Phys. Rev. Lett. **84**, 3795 (2000); Phys. Rev. A **62**, 053404 (2000).
  - [8] H. G. Muller, P. H. Bucksbaum, D. W. Schumacher, and A. Zavriyev, J. Phys. B **23**, 2761 (1990); D. W. Schumacher, F. Weihe, H. G. Muller, and P. H. Bucksbaum, Phys. Rev. Lett. **73**, 1344 (1994).
  - [9] Yi-Yian Yin, Ce Chen, D. S. Elliott, and A. V. Smith, Phys. Rev. Lett. **69**, 2353 (1992).
  - [10] Yi-Yian Yin, D. S. Elliott, R. Shehadeh, and E. R. Grant, Chem. Phys. Lett. **241**, 591 (1995).
  - [11] B. Sheehy, B. Walker, and L. F. DiMauro, Phys. Rev. Lett. **74**, 4799 (1995).
  - [12] E. Dupont, P. B. Corkum, H. C. Liu, M. Buchanan, and Z. R. Wasilewski, Phys. Rev. Lett. **74**, 3596 (1995).
  - [13] A. Haché, Y. Kostoulas, R. Atanasov, J. L. P. Hughes, J. E. Sipe, and H. M. van Driel, Phys. Rev. Lett. **78**, 306 (1997); H. M. van Driel, J. E. Sipe, A. Haché, and R. Atanasov, Phys. Status Solidi (b) **204**, 3 (1997).
  - [14] Takashi Nakajima, Phys. Rev. A **61**, 041403(R) (2000).
  - [15] H. B. Bebb and A. Gold, Phys. Rev. **143**, 1 (1966).
  - [16] A. Burgess and M. J. Seaton, Mon. Not. R. Astron. Soc. **120**, 121 (1960).
  - [17] G. Peach, Mem. R. Astron. Soc. **71**, 13 (1967).
  - [18] H. Helm, N. Bjerre, M. J. Dyer, D. L. Huestis, and M. Saeed, Phys. Rev. Lett. **70**, 3221 (1993).
  - [19] B. P. Shoichiff and E. Weinberger, Can. J. Phys. **57**, 2143 (1979).
  - [20] C. J. Lorenzen and K. Niemax, Phys. Scr. **27**, 300 (1983).